

COMPARISON OF FOUR ANALYTICAL DISPERSION MODELS FOR NEAR-SURFACE RELEASES ABOVE A GRASS SURFACE

KARSTEN HINRICHSSEN

Meteorologisches Institut, University of Hamburg, Bundesstrasse 55, D-2000 Hamburg 13, F.R.G.

(First received 26 July 1984 and received for publication)

Abstract—The results of a new model called 'Pasquill–Businger'-model, and three Gaussian plume models with different diffusion parameters stemming from, (a) the U.S. Nuclear Regulatory Guide 1.145 (1982), (b) the Western German Regulatory Guide 'TA-Luft' (1983), (c) Klug (1969, *Staub-Reinhaltung der Luft* 29, 143–147), are compared with 23 experiments of the Prairie-Grass Project (Barad, 1958, *Geophys. Res. Pap.* 59, AFCRC-TR-58-235). The new model uses the solution of the diffusion equation given by Berlyand (1975, NERC, USEPA), the exchange coefficient for vertical diffusion, K_z , from Businger *et al.* (1971, *J. Atmos. Sci.* 28, 181–189), and Pasquill's (1976, EPA-600/4-76-030 B) relation for σ_y . The new model is superior to the others since it uses power functions for wind velocity and vertical diffusion and is independent of the definition of stability classes.

Key word index: Analytical dispersion model, guidelines, Gaussian plume model.

1. INTRODUCTION

In the western countries the Gaussian plume model (GPM) is used for regulatory purposes. In spite of its shortcomings (see e.g. Gifford, 1976; Pasquill, 1976; Hanna, 1982), the GPM is employed for risk studies (e.g. WASH 1400, German Risk Study for nuclear power stations), for safety analyses (e.g. German Safety Regulatory Guide—draft version), and for accident consequence assessments at chemical (Seveso, Italy) and nuclear (TMI Harrisburg) plants.

Highest ground level concentrations c_g are observed for near-surface releases above surfaces with small roughness length z_0 . These conditions were realized by the Prairie-Grass Project (PGP), reported by Barad (1958). An efficient model should reproduce the PGP-measurements if wake effects behind buildings, settling of heavy gases, and topography can be neglected.

Without deposition, the GPM for continuous emission rates Q is based on the formula

$$c(x, y, z) = \frac{Q(0, 0, H)}{2\pi\bar{u}\sigma_y\sigma_z} \exp\left(-\frac{y^2}{2\sigma_y^2}\right) \left[\exp\left(-\frac{(z-H)^2}{2\sigma_z^2}\right) + \exp\left(-\frac{(z+H)^2}{2\sigma_z^2}\right) \right], \quad (1)$$

where c is the concentration, \bar{u} is a 'characteristic' wind velocity in the x -direction, σ_y and σ_z are the dispersion coefficients in the y - and z -directions, respectively. H is the height of the source, and x , y and z are the coordinates in the direction of the wind, in the cross-wind direction, and vertically upward, respectively. The σ_i ($i = y, z$) are mean values for certain stability classes as defined e.g. by Pasquill (1961), Turner (1964) and Klug (1969). They are functions of x and must be

evaluated from dispersion experiments. Moreover the values of σ_i depend on H and z_0 .

Near to the surface the wind velocity and turbulence strongly depend on height. Therefore it is rather difficult to define constant characteristic values of \bar{u} and σ_i . It is possible however to represent the wind speed $u(z)$ and the vertical exchange coefficient $K_z(z)$ by power laws in the atmospheric surface layer.

Adopting similarity expressions for the vertical concentration profile (e.g. van Ulden, 1978) solutions of the diffusion equation

$$u \frac{\partial c}{\partial x} = \frac{\partial}{\partial z} K_z \frac{\partial c}{\partial z}$$

can be given.

In the next section a model is presented which uses power functions for u and K_z , too. Section 3 describes the data set used for the verification of the 'Pasquill–Businger' model (PBM) and for the tests with three GPMs. Section 4 contains the method of verification, Section 5 nominates the GPMs participating in the test, and Section 6 presents the results.

2. THE 'PASQUILL–BUSINGER' MODEL

Berlyand (1975) published an analytical formula describing the dispersion of pollutants released from point sources:

$$c(x, y, z) = \frac{Q}{\sqrt{2\pi}\sigma_y} \exp\left(-\frac{y^2}{2\sigma_y^2}\right) \exp\left(-\frac{a(z^2 + H^2)}{b\alpha^2 x}\right) \cdot I_{-v}\left(\frac{2a(z \cdot H)^{\alpha/2}}{b\alpha^2 x}\right), \quad (2)$$

where $\alpha = 2 + p - n$, $v = (1 - n)/\alpha$, and I_{-v} is the modified Bessel function of the first kind of order $-v$.

The wind velocity u

$$u(z) = a \cdot z^p \quad (3)$$

with $a = u/z^p$ at $z = z_1$ and the vertical exchange coefficient K_z

$$K_z(z) = b \cdot z^n \quad (4)$$

with $b = K_z/z^n$ at $z = z_2$ are power functions of z .

For K_z the relations given by Businger *et al.* (1971) are adopted since these were derived from measurements over a grass surface (Kansas experiments):

$$K_z(z) = \kappa u_* z / \phi_h(z/L) \quad (5)$$

where

$$\phi_h = 0.85(1 + 6.3z/L) \quad \text{for } 1/L \geq 0 \quad (6a)$$

$$\phi_h = 0.85(1 - 9z/L)^{-1/2} \quad \text{for } 1/L < 0, \quad (6b)$$

ϕ_h is the stability function for heat, $\kappa = 0.4$ is the v. Kármán constant and L the Monin-Obukov length. The relationships of Dyer and Hicks (1970) have been adopted, too.

$$\phi_{hD} = 1 + 5z/L \quad \text{for } 1/L \geq 0 \quad (6c)$$

$$\phi_{hD} = (1 - 16z/L)^{-1/2} \quad \text{for } 1/L < 0. \quad (6d)$$

Pasquill's (1976) relationship for calculating σ_y by

$$\sigma_y = \sigma_\theta \cdot g(x) \cdot x \quad (7)$$

has been used. σ_θ (in radians) is the standard deviation of the lateral wind direction fluctuations and g is a decreasing function of x . The following values of g were used:

x (m)	50	100	200	400	800
$g(x)$	0.95	0.8	0.7	0.65	0.6

Alternatively, the following method has been adopted. Assuming the statistical theory of turbulence, σ_y can be expressed by

$$\sigma_y^2 = \frac{2}{\bar{u}} \int_0^x K_y(x) dx. \quad (8)$$

Values of the exchange coefficient for the lateral diffusion, K_y , are very uncertain. Many authors have determined $K_y = f \cdot K_z$, where f is a function of stability (e.g. Ragland and Dennis, 1975; Segal *et al.*, 1982). In this paper

$$f = \begin{cases} 8 & \text{for } 1/L \geq 0 \\ 16 \frac{x}{50} \left(1 - \frac{50}{L}\right) & \text{for } 1/L < 0, \end{cases} \quad (9)$$

which was derived by comparison of calculated and observed concentrations. K_z and \bar{u} were taken at the height $\bar{z} = 0.5(h + H)$, which is the arithmetic mean of release height H and receiver height h of the horizontal sampling network (see next section). Equation (9) is derived empirically. It is remarkable that for neutral

and stable situations ($L \geq 0$) the assumption of Fickian diffusion is suitable for distances down to $x = 50$ m.

For unstable conditions K_y is a function of L and x . Since for the PGP the smallest distance between the release point and the sampling locations was $x = 50$ m, the value 50 is taken in Equation (9).

3. THE DATA SET USED

During the PGP SO_2 was released for 10 min over a hay field which had a roughness length $z_0 = 0.01$ m. There was no evidence of deposition of the tracer (Barad, 1958). For the horizontal sampling network midjet impingers were mounted at a height $h = 1.5$ m along five semicircular arcs located at $x = 50, 100, 200, 400$ and 800 m distance centered on the point source. The sampling bags were 2 degrees apart. At $x = 800$ m the separation interval was 1 degree.

The vertical sampling network consisted of 6 towers at $x = 100$ m spaced at intervals of 14 degrees. The impingers were mounted at the heights: 0.5, 1.0, 1.5, 2.5, 4.5, 7.5, 10.5, 13.5, 17.5 m.

The meteorological data that were taken included the wind velocity at the heights: 0.25, 0.5, 1.0, 2.0, 4.0, 8.0, 16.0, the air temperature at eight heights up to $z = 16$ m, the mean wind direction and the standard deviation of the wind direction fluctuations for 10 and 20 min periods at $z = 2$ m, φ^{10} and φ^{20} , respectively, at $x = 0$ and $x = 450$ m distant from the source (see Table 1).

A total of 63 experiments were carried out with a release height $H = 0.46$ m. Only those experiments satisfying the two criteria: K1: constant mean wind direction during the experiment, K2: considerable concentrations measured at least at one tower, were accepted for the test. K1 yields maximum concentrations compared with changing mean wind directions and gives a normal shaped distribution of the tracer in the lateral direction. By K2 reliable vertical concentration profiles have been evaluated which turned out to be very useful to rate the models. Applying Klug's (1969) classification scheme, 15 experiments have been excluded from the 29 experiments performed during the neutral stability class 'D'. By examining the Monin-Obukov length L the most stable and unstable experiments of the 'D' class were retained. Thus 23 experiments were kept back having a frequency of stability classes which corresponds to the climatological mean in the middle of Europe.

In Table 1, the stability classes as evaluated from the U.S. Regulatory Guide 1.23 by use of the φ_{450}^{10} value are shown.

One serious problem with Gaussian plume modeling is the determination of the stability classes. The U.S. Nuclear Regulatory Commission uses the Regulatory Guide 1.23 for license purposes. The stability classes are defined by the vertical temperature gradient between two levels or, alternatively, by the standard deviation of the horizontal wind direction. Both result in different stability classes for certain meteorological situations. In the F.R.G. a modified Klug typing scheme is used. It is very similar to 'Pasquill's turbulence types' as reported by Gifford (1976). It differs primarily by use of a more detailed set of rules relating cloudiness, time of day, wind speed and season. Both typing schemes are based on a poorer set of surface layer parameters than the Monin-Obukov length L . This explains the discrepancies between the GMI and NRC classification on the one hand and L on the other hand (see Table 1).

In Table 1, χ_a are the observed values of the normalized concentration at $x = a$, defined by

$$\chi_a = \frac{c(a, 0, h)\bar{u}}{Q(0, 0, H)} \quad (10)$$

Table 1. Some characteristic values of 23 experiments of the Prairie-Grass Project

Exp. nr.	Stab. class		L (m)	φ_0^{10}	φ_0^{20}	$\chi_{50} \cdot 10^5$ (m ⁻²)	φ_{450}^{10}	φ_{450}^{20}	$\chi_{800} \cdot 10^5$ (m ⁻²)	u_* (m s ⁻¹)	p	n
	GMI	NRC										
16	B	B	-5.2	18.5	23.4	455	18.9	18.7	0.2	0.24	0.10	1.40
15	B	D	-7.6	12.8	12.4	1198	11.0	12.4	1.4	0.23	0.13	1.37
43	D	D	-16.0	12.2	13.7	947	10.3	11.7	1.3	0.35	0.13	1.30
44	D	C	-25.0	12.7	13.7	941	14.0	18.1	2.7	0.40	0.14	1.25
19	D	D	-28.0	11.6	12.4	1128	10.1	9.5	1.3	0.39	0.13	1.24
49	C	D	-28.0	11.9	11.1	1171	10.9	10.9	3.5	0.45	0.14	1.24
27	D	D	-30.0	9.2	9.2	1097	8.6	8.5	4.8	0.42	0.17	1.23
26	D	D	-32	13.2	12.1	852	10.2	11.2	2.2	0.43	0.15	1.23
61	D	D	-38	11.0	10.9	1126	9.0	9.5	5.4	0.51	0.13	1.21
30	D	D	-39	10.3	12.3	1180	11.5	10.8	3.9	0.46	0.14	1.21
33	D	D	-51	10.5	9.2	1360	9.0	8.9	4.7	0.50	0.16	1.18
20	C	D	-62	8.3	8.3	1453	7.9	8.2	4.8	0.60	0.15	1.16
45	D	E	-87	6.9	8.2	1712	7.2	8.4	13	0.39	0.15	1.13
57	D	D	-194	8.0	8.2	1725	7.8	8.1	11	0.46	0.16	1.07
22	D	E	204	5.8	5.6	2997	5.1	4.7	34	0.46	0.18	0.90
37	D	E	95	7.0	6.8	2225	7.0	6.6	19	0.29	0.21	0.82
18	D	E	25	5.3	5.7	2987	4.7	4.9	57	0.20	0.31	0.59
59	D	F	11	5.2	4.6	3840	3.6	3.5	198	0.14	0.40	0.42
32	E	E	8.3	3.6	5.2	2935	5.8	3.4	220	0.14	0.47	0.36
36	E	E	7.8	3.8	4.2	2953	4.2	4.4	130	0.10	0.44	0.35
58	E	F	6.4	4.1	4.1	3755	3.3	3.3	256	0.11	0.45	0.31
13	F	F	3.4	3.2	5.0	254	2.4	2.5	148	0.09	0.49	0.22
14	E	F	1.6	3.6	4.3	1072	3.1	5.9	32	0.05	0.67	0.13

L : Monin-Obukov length, φ_0^b : standard deviation of horizontal wind direction fluctuation for a b min interval at $x = a$, χ_a : normalized concentration at $x = a$, u_* : friction velocity, p : wind profile exponent, n : exponent of power function of K_z .

For the most unstable experiment, exp. 16, the ratio χ_{50}/χ_{800} is 2275. For the most stable experiment, exp. 14, the ratio χ_{50}/χ_{800} is only 34.

The values for L and the friction velocity u_* were taken from van Ulden (1978). p and n are the exponents of the power function for u and K_z , respectively, see Equations (3) and (4), with $z_1 = 4$ m and $z_2 = 3$ m. z_2 is not equal to z_1 for practical purposes since $K_z(z)$ was calculated at the intermediate levels of $u(z)$. They were determined from the observed vertical wind profile and from Equation (5) by least square fit methods. For all experiments the approximation was satisfactory. From Table 1 it is seen that p increases with L , whereas n decreases with L . u_* possesses a maximum for neutral conditions and becomes very small in stable situations.

Figure 1 shows $u(z)$ during a typically unstable and stable case. Figure 2 shows $K_z(z)$. In the stable case the K_z -values are only 1 percent of those during the unstable case.

4. THE METHOD OF VERIFICATION

The PGP has been used for verification of many models, e.g. Cramer (1957), Pasquill (1961), Klug (1969), van Ulden (1978), Nieuwstadt and van Ulden (1978). In this paper vertical and horizontal diffusion are investigated simultaneously. By using the observed dispersion parameter, σ_{y0} , in Equation (2), the influence of the vertical diffusion parameterization on the concentration can be proved. With the values gained for K_z the parameterization of σ_y was checked [see Equations (7) and (8)].

Because of criterion K1 the observed horizontal concentration field can be described by the two parameters (χ_0 , σ_{y0}) for each of the five semicircles. χ_0 and σ_{y0} are the amplitude and standard deviation, respectively, of the Gaussian distribution of the plume evaluated from the measurements by least square fit methods.

The determination of K_z and σ_y was done with a subgroup

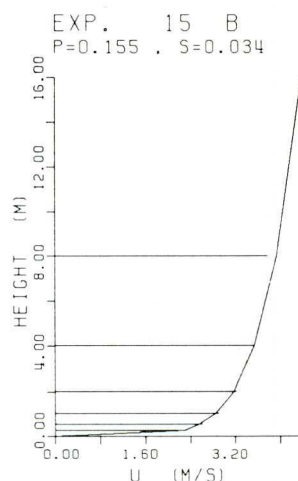


Fig. 1a. Approximated wind velocity profile and observations (horizontal bars) for exp. 15, unstable conditions. p is the exponent of the power function of u , s is the root mean square error of the approximated profile.

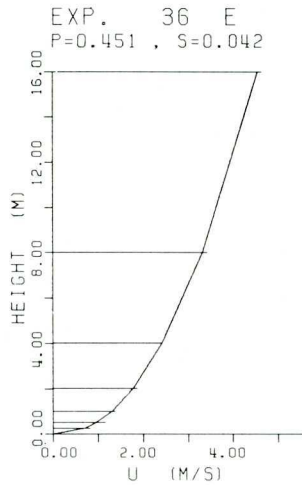


Fig. 1b. Approximated wind velocity profile and observations (horizontal bars) for exp. 36, stable conditions. p is the exponent of the power function of u , s is the root mean square error of the approximated profile.

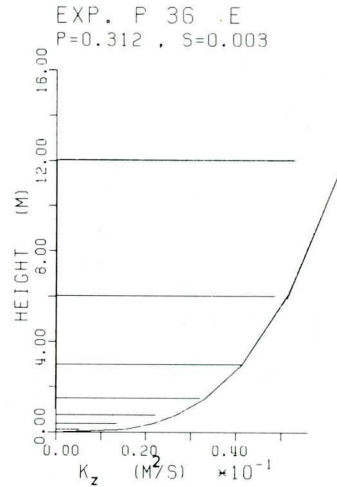


Fig. 2b. Approximated K_z profile and values as calculated by the function of Businger (horizontal bars) for exp. 36, stable conditions. p is the exponent of the power function of K_z , s is the root mean square error of the approximated profile.

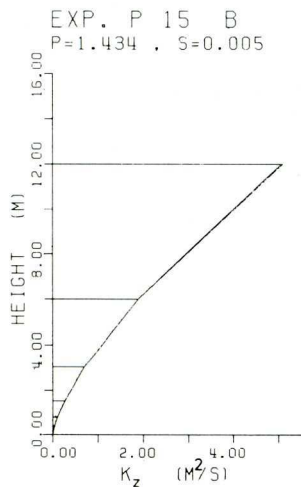


Fig. 2a. Approximated K_z profile and values as calculated by the function of Businger (horizontal bars) for exp. 15, unstable conditions. p is the exponent of the power function of K_z , s is the root mean square error of the approximated profile.

of the 23 PGP experiments, i.e. the 10 experiments: 15, 49, 43, 57, 22, 18, 32, 36, 58, 13 (Dunst *et al.*, 1984).

The relative error $r.e.$ was defined by

$$r.e. = \frac{f_c - f_0}{f_c}, \quad (11)$$

where f stands for χ and σ_y , respectively. f_c means the calculated value and f_0 is the observed quantity.

Assuming $r.e.$ is normally distributed this definition has the following advantage: To obtain, for example, a 95 percent

probability not to underestimate the observed concentration χ_0 the calculated concentration χ_c must be multiplied by a 'security' factor

$$\varepsilon = 1 - (\bar{r.e.} - 2s), \quad (12)$$

where $\bar{r.e.}$ is the mean relative error and s is the standard deviation of $r.e.$ Generally $\bar{r.e.}$ and s are functions of x .

The calculations were repeated for the remaining 13 experiments, showing that the values of $\bar{r.e.}$, s , and r were only slightly different. Therefore, only the statistics for the whole set of experiments are presented in section 6.2.

5. GAUSSIAN PLUME MODELS

The concentrations calculated by the 'Pasquill-Businger' model (PBM) are compared with those of three Gaussian plume models (GPMs) which differ from the turbulence typing schemes and from the parameter sets for the dispersion parameters σ_i . The following GPMs were examined:

1. The set of Klug (1969) which was derived from the PGP.
2. The Regulatory Guide 1.145 (NCR) of the U.S. Nuclear Regulatory Commission (1982) with σ_i following Eimutis and Konicek (1972). The stability classes were determined from R.G. 1.23.
3. The Regulatory Guide 'TA-Luft' (GMI) of the Western German Ministry of the Interior (1983). The dispersion coefficients were determined from experiments done at the Jülich Nuclear Research Center, F.R.G. The release height was 50 m. These dispersion coefficients have been accepted by the F.R.G. Regulatory staff with the objective of assessing the risk to public health and safety resulting from the operation of facilities.

6. RESULTS

6.1. Case studies

In Fig. 3 the horizontal concentration distribution as calculated by the PBM and the GPMs is compared with the observations at 5 semicircles. Figure 3a is an example for a very unstable situation ($L = -7.6$). Figure 3b stands for a very stable case ($L = 7.8$). Figures 4a and 4b show the vertical distribution at the towers, the positions of which are indicated by the arrows in Fig. 3. As Elliot (1961) pointed out for unstable situations, the vertical concentration has an exponential and not a Gaussian distribution. The most outstanding advantage of the PBM compared with the GPMs is its ability to predict the vertical distribution of the tracer reliably.

In Fig. 5a the normalized concentration χ_c as calculated by the PBM is plotted against the observed χ_0 -values for the 23 experiments at a source distance $x = 200$ m. Figure 5b (Fig. 5c) applies to the R.G. 1.145 (TA-Luft).

Another advantage of the PBM is that it does not need a stability classification as the GPMs do. The definition of stability classes by some (meteorological) parameters is not very satisfactory which can be read from the fact that there do exist more than 20 different turbulence typing schemes.

Table 2 compares the χ_c values of the four models

with the observations at $x = 800$ m. The relative error *r.e.* is given for each experiment. It must be emphasized that the use of the guidelines gives rise to an underestimation of the peak concentration for near-surface releases over smooth surfaces in stable conditions. Particularly, the concentrations as calculated by the GMI parameter set are too small since the roughness length of the Jülich test site is $z_0 = 1$ m. A small value of the standard deviation s indicates that the error of the model will be small if it is applied to individual cases such as accidental releases.

6.2. Statistics

In this section the mean relative error $\overline{r.e.}$, the standard deviation s , and the correlation coefficient r of the dispersion models are reported for the ensemble of 23 experiments and each of the five distances.

6.2.1. *Vertical diffusion parameterization.* Table 3 shows the efficiency of the vertical diffusion parameterization by setting $\sigma_y = \sigma_{y0}$ in Equations (1) and (2). Of course, errors from the model assumptions are included also since observed and calculated concentrations at $z = 1.5$ m have been compared. In the first two columns the K_z -relationships of Businger *et al.* (1971) and Dyer and Hicks (1970) are compared. Only for $x = 50$ m are the Dyer values superior to those of Businger. From this fact, the conclusion of Dyer (1974)

Table 2. Comparison of calculated and observed normalized concentrations for 23 experiments at $x = 800$ m

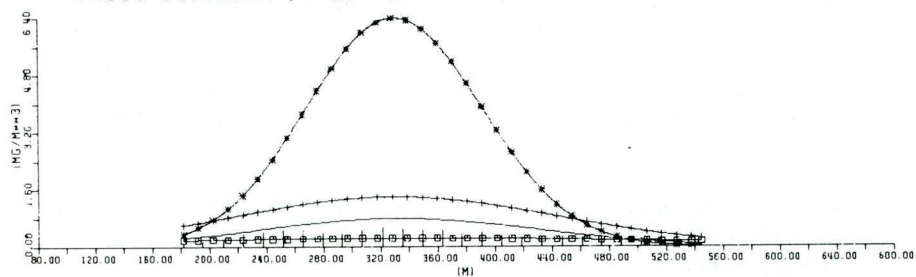
Distance of semicircle: 800 m											
Norm. conc.											
Exp.	Stab.	Observation	Calculation	<i>r.e.</i>	GMI	<i>r.e.</i>	NRC	<i>r.e.</i>	KLUG	<i>r.e.</i>	
nr.	class (Klug)										
16	B	0.2	1.0	0.83	0.7	0.77	4.3	0.96	4.2	0.96	
15	B	1.4	2.4	0.41	0.7	−0.98	19.4	0.93	4.2	0.67	
43	D	1.3	4.6	0.71	3.3	0.60	19.4	0.93	48.5	0.97	
44	D	2.7	4.4	0.39	3.3	0.20	7.3	0.64	48.5	0.95	
19	D	1.3	6.4	0.79	3.3	0.60	19.4	0.93	48.5	0.97	
49	C	3.5	5.8	0.41	1.7	−1.02	19.4	0.82	16.8	0.79	
27	D	4.8	7.2	0.34	3.3	−0.44	19.4	0.76	48.5	0.90	
26	D	2.2	6.5	0.66	3.3	0.33	19.4	0.89	48.5	0.95	
61	D	5.4	8.4	0.36	3.3	−0.63	19.4	0.72	48.5	0.89	
30	D	3.9	6.6	0.41	3.3	−0.18	19.4	0.80	48.5	0.92	
33	D	4.7	9.2	0.49	3.3	−0.43	19.4	0.76	48.5	0.90	
20	C	4.8	11.3	0.58	1.7	−1.80	19.4	0.75	16.8	0.72	
45	D	13.0	13.5	0.04	3.3	−2.93	39.5	0.67	48.5	0.73	
57	D	10.6	14.8	0.28	3.3	−2.22	19.4	0.45	48.5	0.78	
22	D	34.2	31.7	−0.08	3.3	−9.35	39.5	0.14	48.5	0.30	
37	D	18.9	26.0	0.27	3.3	−4.73	39.6	0.52	48.5	0.61	
18	D	57.0	53.0	−0.08	3.3	−16.25	39.5	−0.44	48.5	−0.17	
59	D	197.9	93.3	−1.12	3.3	−58.96	88.8	−1.23	48.5	−3.08	
32	E	220.3	57.3	−2.85	5.5	−38.94	39.6	−4.57	102.7	−1.15	
36	E	130.1	89.0	−0.46	5.5	−22.59	39.5	−2.29	102.6	−0.27	
58	E	256.3	129.3	−0.98	5.5	−45.50	88.8	−1.89	102.6	−1.50	
13	F	147.5	183.9	0.20	10.0	−13.70	88.8	−0.66	290.0	0.49	
14	E	32.2	211.3	0.85	5.5	−4.85	88.8	0.64	102.6	0.69	
Mean value		$\overline{r.e.}$		0.107		−9.695		0.054		0.349	
Standard deviation		<i>s</i>		0.824		16.538		1.371		1.003	
Correlation coeff.		<i>r</i>		0.943		0.750		0.890		0.767	

r.e.: Relative error; GMI: German Regulatory Guide; NRC: U.S. Regulatory Guide 1.145; Businger: new model.

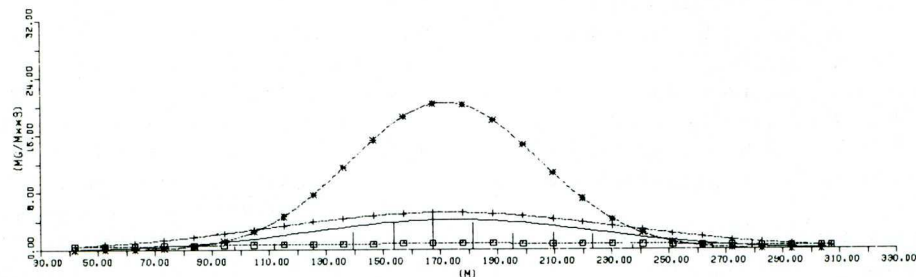
EXP. P 15 B

SOURCE STRENGTH : 95500 MG/SEC SO₂

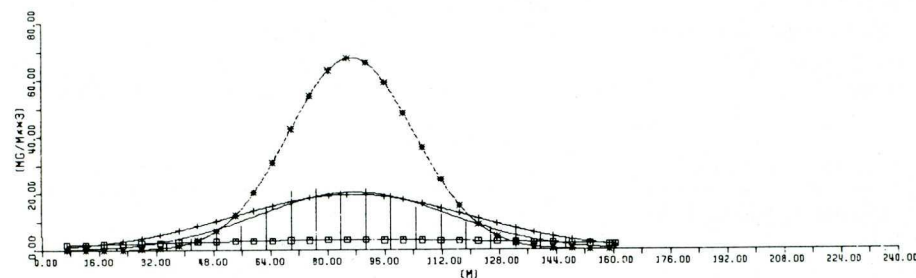
— PASQU-BUSINGER , -□-□- GMI , -x-x-x- NRC , -+--+ KLUG



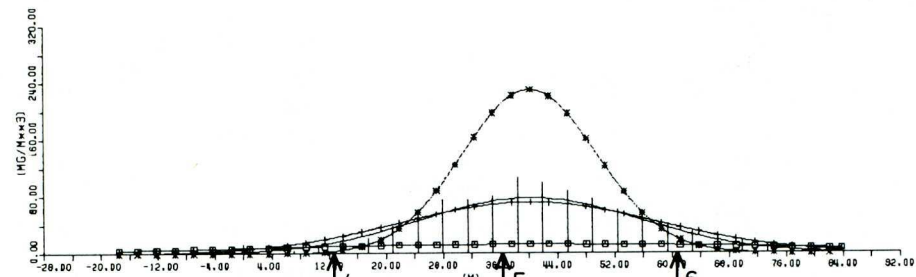
ARC 5 , DISTANCE : 800 M



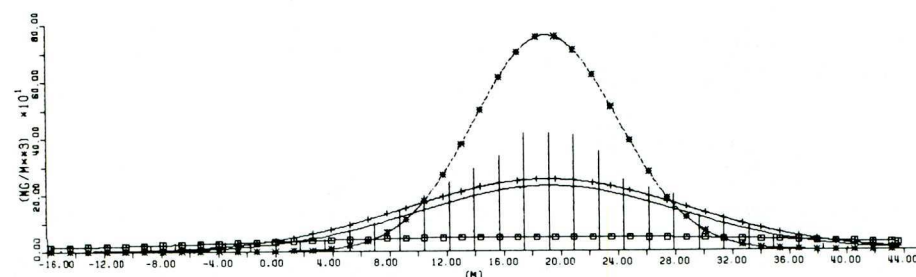
ARC 4 , DISTANCE : 400 M



ARC 3 , DISTANCE : 200 M



ARC 2 , DISTANCE : 100 M



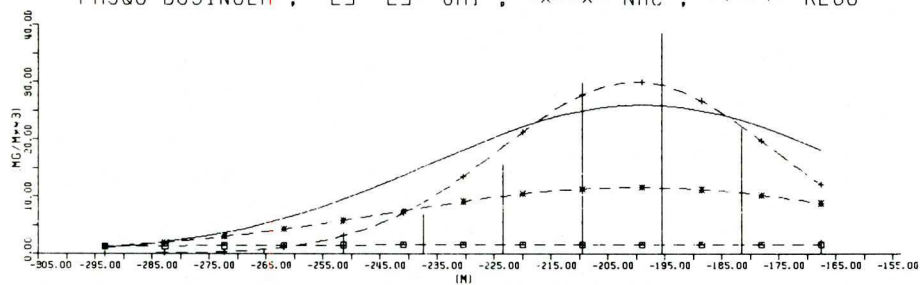
ARC 1 , DISTANCE : 50 M

Fig. 3a. Horizontal concentration χ_c as calculated by four models and observations (vertical bars) at $z = 1.5$ m for exp. 15, unstable situation. The arrows indicate the positions of the towers.

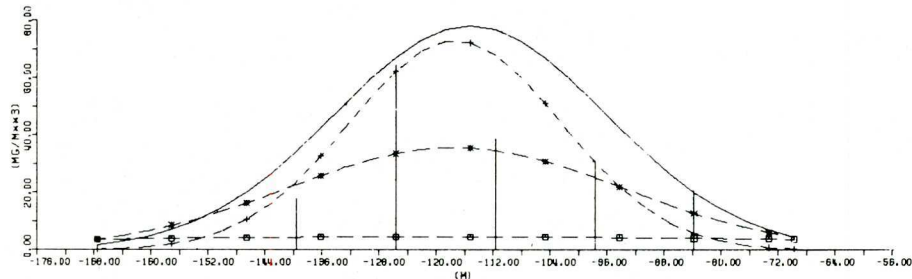
EXP. P 36 E

SOURCE STRENGTH : 40000 MG/SEC SO₂

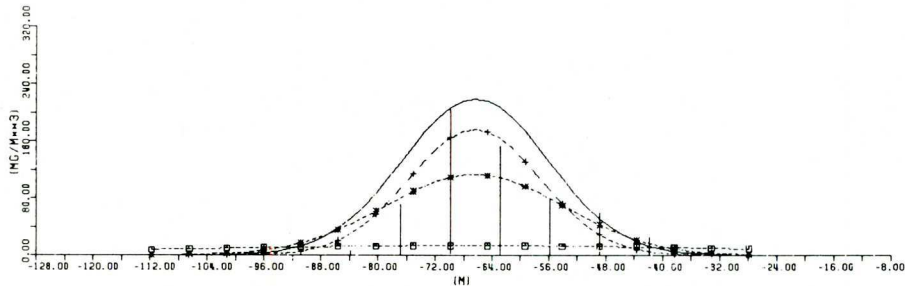
— PASQU-BUSINGER , -□--□- GMI , -x--x- NRC , -+--+ KLUG



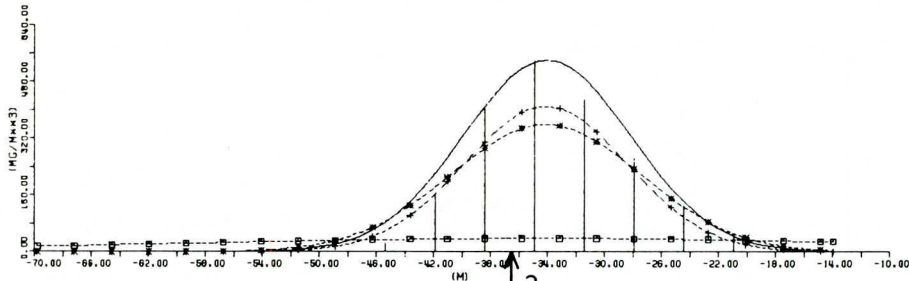
ARC 5 , DISTANCE : 800 M



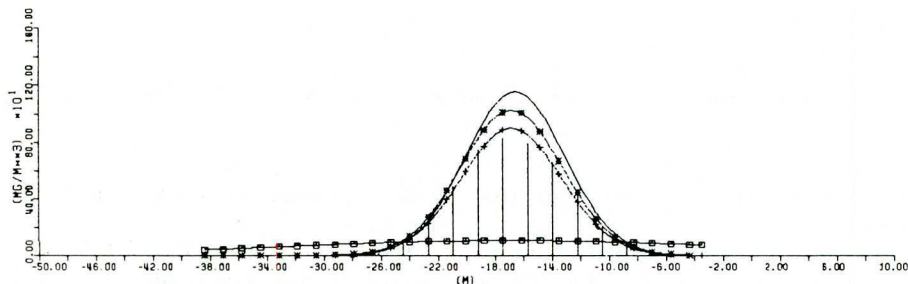
ARC 4 , DISTANCE : 400 M



ARC 3 , DISTANCE : 200 M



ARC 2 , DISTANCE : 100 M



ARC 1 , DISTANCE : 50 M

Fig. 3b. Horizontal concentration χ_c as calculated by four models and observations (vertical bars) at $z = 1.5$ m for exp. 36, stable situation. The arrow indicates the position of the tower.

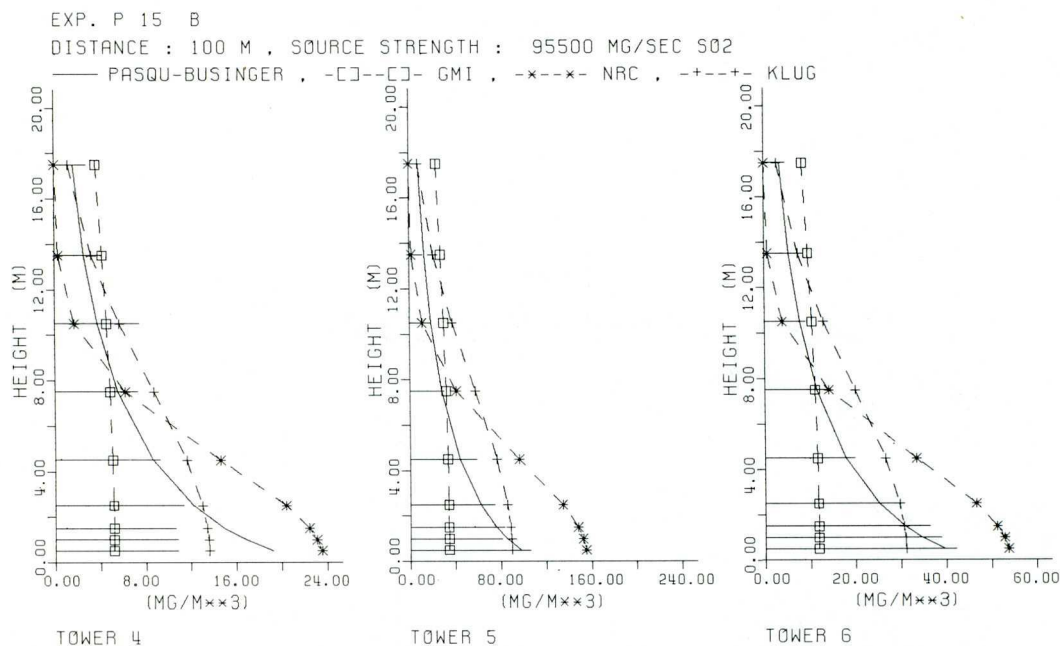


Fig. 4a. Vertical concentration χ_c as calculated by four models and observations (horizontal bars) at $x = 100$ m for exp. 15, unstable situation.

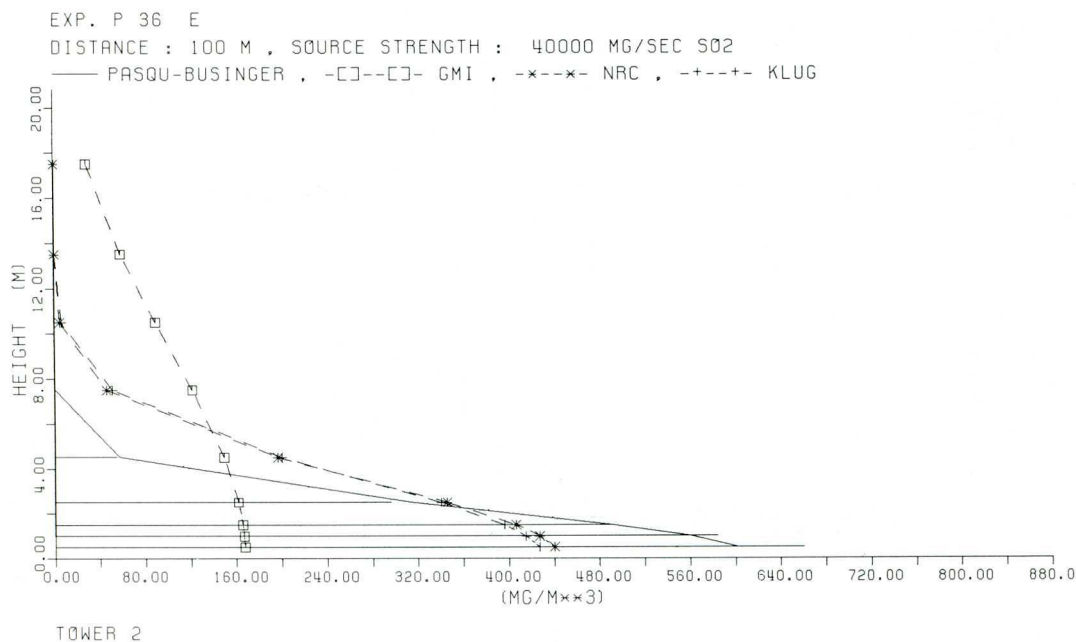


Fig. 4b. Vertical concentration χ_c as calculated by four models and observations (horizontal bars) at $x = 100$ m for exp. 36, stable situation.

has to be reemphasized, that it is not clear which of the two is the more reliable.

The correlation factor r reaches up to 0.99 for the Businger relation but r is not a good tool to rate the validity of a dispersion model (see the last column of Table 3). Adopting a similarity theory solution (van Ulden, 1978), computed crosswind integrated concen-

trations compare favourably with the TGT experimental data

The σ_z -values of the NRC and Klug models are suitable, but the vertical diffusion calculated by the GMI-model is too large. The scattering as indicated by the standard deviation s is also considerable. It should be stated that the σ_z -values of the GPMs were de-

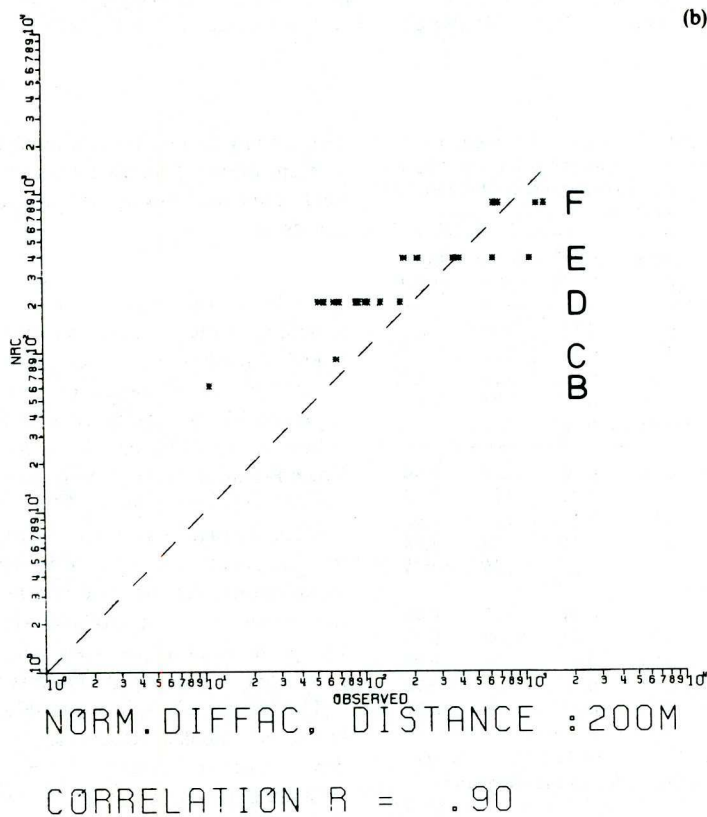
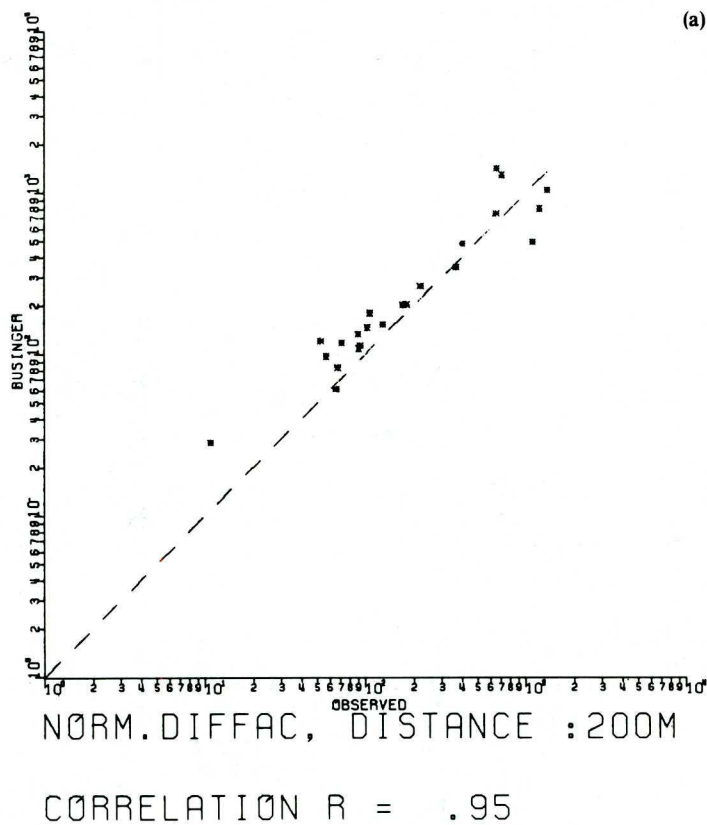


Fig. 5 (a and b).

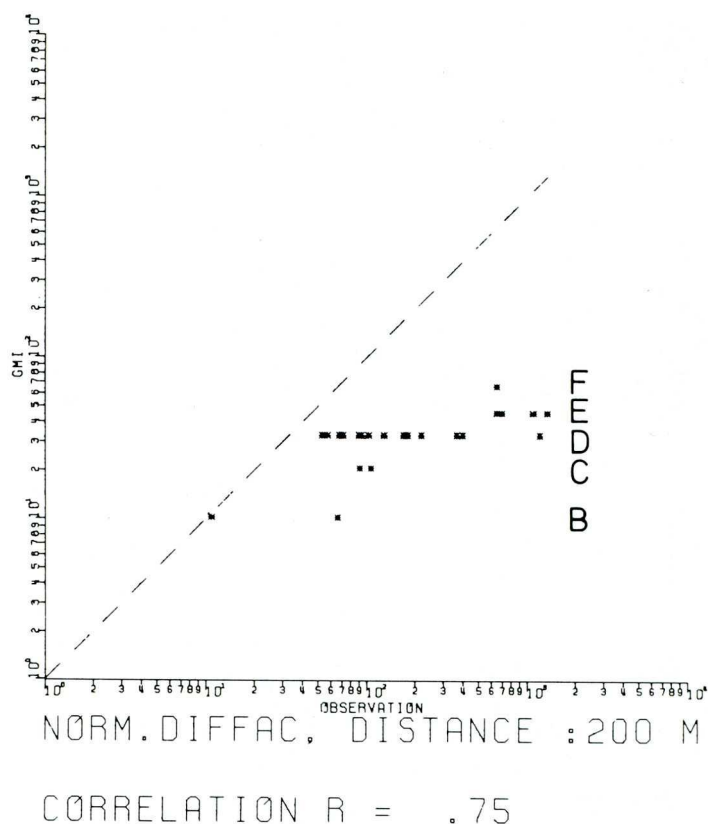


Fig. 5. Comparison of calculated χ_c and observed χ_o normalized concentration for 23 experiments at $x = 200$ m. (a) Pasquill-Businger model, (b) Regulatory Guide 1.145 (NRC), (c) Regulatory Guide 'TA-Luft' (GMI).

Table 3. Mean relative error $\bar{r.e.}$, standard deviation s , and correlation coefficient r of the vertical dispersion parameterization of five models, if $\sigma_y = \sigma_{y0}$, 23 experiments of the Prairie-Grass Project

	x (m)	Businger (1973)	Dyer (1970)	NRC (1982)	Klug (1969)	GMI (1983)
$\bar{r.e.}$	50	-0.09	0.0	0.12	0.05	-1.22
	100	0.04	0.16	0.12	0.10	-1.55
	200	0.13	0.37	0.17	0.21	-1.57
	400	0.22	0.36	0.26	0.34	-1.37
	800	0.31	0.44	0.38	0.46	-1.15
s	50	0.31	0.26	0.26	0.24	0.64
	100	0.17	0.15	0.21	0.26	0.73
	200	0.17	0.17	0.26	0.29	0.93
	400	0.23	0.26	0.41	0.39	1.28
	800	0.27	0.30	0.52	0.45	1.74
r	50	0.49	0.49	0.49	0.47	0.40
	100	0.99	0.97	0.98	0.98	0.97
	200	0.98	0.96	0.94	0.98	0.96
	400	0.83	0.77	0.70	0.81	0.74
	800	0.97	0.95	0.94	0.95	0.93

Businger, Dyer: K_z -relationship of Businger *et al.* (1971) and Dyer and Hicks (1970) used in the Berlyand (1975) solution, Equation (2). NRC, Klug, GMI: σ_z -values of R.G. 1.145, Klug (1969), 'TA-Luft' used in the Gaussian plume model, Equation (1).

terminated by means of reproducing the observed surface concentrations. Therefore, the results of the GPMs are very doubtful if they are adopted for elevated receiving points.

6.2.2. Lateral diffusion parameterization. Corresponding to the previous section, the reliability of five lateral diffusion parameter sets is studied. Table 4 points out that Equation (9) and Pasquill's formula, Equation (7), are quite satisfactory whereas the σ_y -values of the NRC and Klug models are too small. From Equation (11) it is clear that the GMI-values are considerably too large.

6.2.3. Normalized concentrations. Table 5 summarizes the effective error of the examined models, i.e. assumptions inherent in Equations (1) and (2) and both the vertical and horizontal diffusion parameterization. By the choice of the 23 experiments, see Section 3, it is concluded that observational errors are negligible.

The 'Pasquill-Businger'-model is superior since scattering is smallest. According to Equation (12) the largest 'security' factor, $\epsilon_{800} = 2.5$, is yielded at $x = 800$ m. However, the Klug model ($\epsilon_{800} = 2.7$) and the NRC model ($\epsilon_{800} = 3.2$) in connexion with the turbulence typing scheme of R.G. 1.23 are reliable, too.

Table 4. Mean relative error $\overline{r.e.}$, standard deviation s , and correlation coefficient r of the lateral diffusion parameterization for 23 experiments of the Prairie-Grass Project

	x (m)	Equation (9)	GMI (1983)	NRC (1982)	Klug (1969)	Pasquill (1976)
$\overline{r.e.}$	50	-0.16	0.52	-0.59	-0.55	-0.16
	100	-0.11	0.49	-0.48	-0.62	-0.16
	200	-0.08	0.47	-0.39	-0.68	-0.14
	400	-0.29	0.44	-0.41	-0.94	-0.22
	800	-0.18	0.38	-0.36	-0.97	-0.06
s	50	0.36	0.22	0.39	0.62	0.41
	100	0.31	0.27	0.49	0.77	0.36
	200	0.32	0.32	0.57	0.99	0.35
	400	1.02	0.34	0.73	1.32	0.86
	800	0.69	0.45	0.79	1.36	0.50
r	50	0.81	0.13	0.84	0.55	0.77
	100	0.89	0.14	0.86	0.61	0.81
	200	0.92	0.14	0.90	0.68	0.87
	400	0.82	0.20	0.78	0.44	0.69
	800	0.91	0.30	0.84	0.64	0.81

Table 5. Mean relative error $\overline{r.e.}$, standard deviation s , and correlation coefficient r of the normalized concentration χ_c as calculated by the 'Pasquill-Businger' model and three Gaussian plume models

	x (m)	'Pasquill-Businger'	GMI (1983)	NRC (1982) R.G. 1.23	NRC (1982) Gifford	Klug (1969)
$\overline{r.e.}$	50	-0.04	-4.4	0.40	0.17	0.26
	100	0.09	-6.6	0.31	-0.06	0.20
	200	0.14	-8.0	0.21	-0.29	0.22
	400	0.19	-8.2	0.22	-0.39	0.32
	800	0.11	-9.7	0.05	-0.64	0.35
s	50	0.34	2.9	0.22	0.49	0.40
	100	0.33	6.5	0.41	0.83	0.64
	200	0.40	9.5	0.61	1.32	0.77
	400	0.54	12.5	0.86	1.89	0.88
	800	0.82	16.5	1.37	2.56	1.00
r	50	0.40	0.21	0.39	0.25	0.22
	100	0.97	0.71	0.93	0.72	0.73
	200	0.95	0.74	0.90	0.72	0.76
	400	0.97	0.74	0.91	0.74	0.77
	800	0.94	0.75	0.89	0.71	0.77

If the NRC-model is used with the turbulence typing scheme based on synoptic meteorological data (see Gifford, 1976), concentrations are underestimated. The GMI model predicts concentrations which are too small. This is primarily a consequence of too large σ_y -values.

Looking at the different physical assumptions included in the models the following may be stated: (i) The PBM is superior since it allows for power functions of u and K_z . This corresponds with observations in the constant flux layer. (ii) The Pasquill parameters used in the NRC-model are more suitable if the

stability classification is based on the 'turbulence related quantity σ_θ ' rather than on synoptic meteorological data. (iii) The GMI-model is not satisfactory since its parameters were derived from experiments at a site having a roughness length $z_0 = 1$ m.

6.3. Availability of the 'Pasquill-Businger' model

The PBM was verified only for the interval $50 < x < 800$ m over a very smooth surface. Detailed case studies yielded two shortcomings of the PBM: in extremely stable situations (see exp. 14 in Table 1), K_z cannot be described by a power function since the maximum value of K_z occurs at very low heights.

Secondly, in extremely unstable cases (see exp. 16 in Table 1), most of the tracer escapes the Prandtl-layer after a short travel distance. However the power functions of u and K_z were calculated from data taken at the lowest 16 m. Besides, the Businger relation for K_z is questionable in very unstable situations (Deardorff and Willis, 1974).

For these reasons the 'Pasquill-Businger' model should be used for $-0.15 \leq 1/L \leq 0.2$ only.

7. CONCLUSIONS

The results of a model, called 'Pasquill-Businger' model (PBM), have been compared with Gaussian plume models. The PBM is independent of the definition of stability classes and uses power functions for K_z and u , and the Pasquill (1976) formula for σ_y . It was verified from 10 experiments and examined by another 13 experiments of the Prairie-Grass series and found superior to the Gaussian plume models—the vertical distribution of the tracer is especially very well calculated by the PBM. It should be used in guidelines and safety studies for near-surface releases over smooth surfaces only, but these are the most dangerous emergency situations. Its application makes it necessary to determine the specific local surface layer parameters which could be obtained by the applicants for construction permits and operating licenses.

REFERENCES

- Barad M. L. (1958) Project Prairie-Grass, a field program in diffusion. Vols I and II. *Geophys. Res. Pap.* **59**, AFCRC-TR-58-235.
- Berlyand M. Y. (1975) Contemporary problems of atmospheric diffusion and pollution of the atmosphere. Translated version by NERC, USEPA, Raleigh, NC.
- Businger J. A., Wyngaard J. G., Izumi Y. and Bradley E. F. (1971) Flux-profile relationships in the atmospheric surface layer. *J. Atmos. Sci.* **28**, 181-189.
- Cramer H. E. (1957) A practical method for estimating the dispersal of atmospheric contaminants. *Proceedings of the 1st National Conference on Appl. Met.*, pp. C33-C55. Ann. Met. Soc., Hartford, Conn.
- Deardorff J. W. and Willis G. E. (1974) Computer and laboratory modeling of the vertical diffusion of non-buoyant particles in the mixed layer. *Adv. Geophys.* **18(B)**, 187-200. Academic Press, N.Y.

- Dunst M., Hinrichsen K., Fischer I. and Fehmer M. (1984) Untersuchung der Ausbreitung von Luftverunreinigungen bei Störfällen. West German Federal Environmental Agency, Berlin, Project-No. 104 09 203.
- Dyer A. J. (1974) A review of flux-profile relationships. *Boundary-Layer Met.* **7**, 363–372.
- Dyer A. J. and Hicks B. B. (1970) Flux-gradient relationships in the constant flux layer. *Q. Jl R. met. Soc.* **96**, 715–721.
- Eimutis E. C. and Konicek M. G. (1972) Derivations of continuous functions for the lateral and vertical atmospheric dispersion coefficients. *Atmospheric Environment* **6**, 859–863.
- Elliot W. P. (1961) The vertical diffusion of gas from a continuous source. *Int. J. Air Wat. Pollut.* **4**, 33–46.
- German Ministry of the Interior (1983) Technische Anleitung Luft, Regulatory Guide, 23 Feb. 1983, GMBI.
- Gifford F. A. (1976) Turbulent diffusion-typing schemes: a review. *Nuc. Saf.* **17**, 68–86.
- Hanna S. R. (1982) Review of atmospheric diffusion models for regulatory applications. Techn. Rep. 177. World Meteorological Organization.
- Klug W. (1969) Ein Verfahren zur Bestimmung der Ausbreitungsbedingungen aus synoptischen Beobachtungen. *Staub-Reinhaltung der Luft* **29**, 143–147.
- Nieuwstadt F. and van Ulden A. P. (1978) A numerical study of the vertical dispersion of passive contaminants from a continuous source in the atmospheric surface layer. *Atmospheric Environment* **12**, 2119–2124.
- Pasquill F. (1961) The estimation of the dispersion of windborne material. *Met. Mag.* **90**, 33–49.
- Pasquill F. (1976) Atmospheric dispersion parameters in Gaussian plume modelling. Part II. Possible requirements for change in the Turner workbook values. EPA-600/4-76-030 B.
- Ragland K. W. and Dennis R. L. (1975) Point source atmospheric diffusion model with variable wind and diffusivity profiles. *Atmospheric Environment* **9**, 175–189.
- Segal M., Mahrer Y. and Pielke R. A. (1982) A numerical model study of plume fumigation during nocturnal inversion break-up. *Atmospheric Environment* **16**, 513–519.
- Turner B. D. (1964) A diffusion model for an urban area. *J. appl. Met.* **3**, 83–91.
- U.S. Nuclear Regulatory Commission (1972) Onsite meteorological programs. Regulatory Guide 1.23 (Safety Guide 23), USNRC, Wash., DC, 20555.
- U.S. Nuclear Regulatory Commission (1982) Atmospheric dispersion models for potential accident consequence assessments at nuclear power plants. Reg. Guide 1.145, USNRC, Wash., DC, 20555.
- Van Ulden A. P. (1978) Simple estimates for vertical diffusion from sources near the ground. *Atmospheric Environment* **12**, 2125–2129.